UNSYS digital

Journal of Unmanned System Technology

Fault-Tolerant Control of Quadrotor Helicopter Using Gain-Scheduled PID and Model Reference Adaptive Control

Iman Sadeghzadeh, Ankit Mehta, and Youmin Zhang

Department of Mechanical and Industrial Engineering, Concordia University, Canada

Abstract—This paper presents development, implementation, experimental testing and comparison of two useful control approaches to a quadrotor Unmanned Aerial Vehicle (UAV) test-bed available at Concordia University for the purpose of enhancing reliability, safety and Fault-Tolerant Control (FTC) of the UAV. A Gain-Scheduled Proportional-Integral-Derivative (GS-PID) controller and a Model Reference Adaptive Control (MRAC) scheme are the main control techniques investigated in this paper based on their wide and popular applications in many engineering systems. Controllers are designed and implemented on the on-board single-chip micro-computer in order to keep the desired height of the helicopter in both normal (faultfree) and faulty flight conditions. In the MRAC case, in addition to height control, some other faulty cases are also considered for the trajectory tracking control with typical trajectories such as square shape trajectory. Finally, comparison results based on experimental testing of the two types of controllers on the UAV test-bed are presented. From the operational point of view, MRAC showed a promising performance for handling the fault imposed to all actuators as well as good fault-free control performance. On the other hand, the GS-PID controller with a linear transition between modes was able to react in a faster way than MRAC to maintain good control of the quadrotors height if the controller reaction/switching time is kept as short as possible. In other words, the GS-PID showed stronger fault-tolerant control capability than MRAC to keep the height of the helicopter if the switching time of the GS-PID controller gains after fault occurrence is kept close to zero.

Keywords—Fault-tolerant control, Unmanned Aerial Vehicle (UAV), Gain-Scheduled Proportional-Integral-Derivative (GS-PID) control, Model Reference Adaptive Control (MRAC), actuator faults.

I. Introduction

Safety, reliability and acceptable level of performance of dynamic control systems are key performance measures in control systems not only in normal operation conditions but also in the presence of partial faults or total failures in the components of the controlled system. Hence, the role of Fault-Tolerant Control System (FTCS) is revealed evidently. In fact, when a fault occurs in a system, it suddenly starts to behave in an unanticipated manner. So, the fault-tolerant controller should be able to handle the fault/damage and to guarantee system stability and acceptable performance in the presence of faults/damages [1]. Since this work is dealing with faulttolerant control, the terminological distinction between fault and failure can be defined as follows [2]: "A fault is an unpermitted deviation of at least one characteristic property (feature) of the system from the acceptable, usual, standard condition" and "A failure is a permanent interruption of a system's ability to perform a required function under specified operating conditions".

Faults and failures can be investigated for both sensors and actuators. This work is dealing with only actuator faults, and sensor faults are out of the scope of this work, although the FTC strategies can also be directly applied to the sensor faults case. Actuator's faults can be in the form of floating around a trim condition, locked-in-place, hard-over and loss of control effectiveness. Actuator faults can also occur in additive or multiplicative manner to the actuator. There are different techniques to handle such faults. Some recent popular techniques used for this reason are such as: multiple model switching and tuning, multiple model adaptive control, control allocation and re-allocation, Interacting Multiple Model (IMM), Model Predictive Control (MPC), Sliding Mode Control (SMC), neural network, eigenstructure assignment and Model Reference Adaptive Control (MRAC), Gain Scheduling (GS) and Linear Parameter Varying (LPV), etc. [3].

Although a reconfigurable control strategy based on GS was initially proposed by Moerder et al. (1989) which used a linear quadratic optimization-based simultaneous stabilization algorithm for each individual controller, gain-scheduled PID (GS-PID) control does not investigated in the literature. In view of the wide use of PID for industrial applications for normal operating conditions and the power for using GS strategy for handling fault cases, it motivated the investigation and development of GS-PID in this current work with the hope that GS-PID can be a practical and widely used FTC strategy as PID for safety-critical systems with fault-tolerance capability. Based on the above motivation, a set of individual PID controllers are designed and tuned to control the quadrotor helicopter UAV under the faultfree and faulty flight conditions. Gain-scheduling strategy is then combined with PID controllers for achieving fault-tolerant control of the quadrotor helicopter under different fault operating conditions. In [4] a GS-PID fault/damage tolerant control according to the measured airspeed is applied to a twin-engine fixed-wing UAV airplane as well as a fault-tolerant control simulation work for a

Corresponding author: Y. Zhang (e-mail: Youmin.Zhang@concordia.ca)
This paper was submitted on December 1, 2015; revised on December 9, 2015; and accepted on December 27, 2015.
DOI: 10.21535/just.v3i3.64

quadrotor UAVs in [5]. In [6] a fuzzy PID controller is used to handle the partial actuator's fault for the quadrotor helicopter UAV. In [7], a fast response design based PID controller for hovers is presented using Ziegler-Nichols tuning approach. The results in simulation show the effectiveness of the designed controller. In [8] a comparison between a PID controller and a Linear Quadratic (LQ) controller applied on a simplified quadrotor dynamics model is presented. The LQ controller is applied to a more complete model. A robust PID controller is for attitude stabilization of a quadrotor UAV [9].

On the other hand, adaptive control techniques are one of recently widely developed and used techniques for handling fault situations as one of model-based control strategies. In fact, adaptive control is originally a control technique which is based on a concept that controllers must adapt to a controlled system with parameters which vary, or are initially uncertain. According to [10] "An adaptive system is any physical system that has been designed with an adaptive viewpoint" and "an adaptive controller is a controller with adjustable parameters and a mechanism for adjusting the parameters". As one of adaptive control techniques, Model Reference Adaptive Control (MRAC) is concerned with forcing the dynamic response of the controlled system to asymptotically approach that of reference system, despite parametric uncertainties in the plant[11]. MRAC consists of an ordinary feedback loop composed of the process and the controller and another feedback loop that changes the controller parameters. The parameters are changed on the basis of feedback from the error, which is the difference between the output of the system and the output of the reference model. In [12] a comparison is made for different MRAC approaches applied to the NASA Generic Transport Model (GTM) which is a subscale model of Boeing 757 fixed-wing UAV. Also in [13] a multivariable MRAC is applied to the same test-bed. Another example for MRAC with application to civil aviation application for a real scale Bonanza fly-by-wire airplane is presented in [14]. In [15], a modified MIT rule is designed for a second- order system and results have been shown in simulation environment. A similar work for a second-order system is described in [16]. A MRAC fuzzy controller design and application to an automatic gauge control system is presented in [17]. For fast parameter adaption, an optimal control modification approach for MRAC is developed in [18]. In [19] a new direct model reference fuzzy adaptive control of SISO continuous-time nonlinear systems based on an adaptive Takagi-Sugeno (TS) fuzzy system is developed. Finally, a combination of feedback linearization with indirect MRAC technique is presented in [20].

During recent years, UAVs have proved to play a significant role in the world of aviation. Among the rotorcrafts, quadrotor helicopters can usually afford a larger payload than conventional helicopters due to their four rotors configuration. Moreover, small quadrotor helicopters possess a great manoeuvrability and are potentially simpler to manufacture. For these advantages, quadrotor helicopters have received much and increased interests in UAV research and development. The quadrotor helicopter is an under-actuated system with six outputs and four inputs and the states are highly coupled. There are four fixed-pitch-angle blades whereas single-rotor helicopters have variable-pitch-angle (collective) blades. Control of a quadrotor helicopter is performed by varying the speed of each rotor. The configuration and structure of a quadrotor, especially the Quanser quadrotor unmanned helicopter (as known also Qball-X4) which was developed in collaboration between Concordia University and Quanser Inc. through an NSERC (Natural Sciences and Engineering Research Council of Canada) Strategic Project Grant (SPG) led by Concordia University, are presented in this paper, with related hardware/software of the quadrotor helicopter, as well as development, implementation and experimental testing and comparison of the two controllers GS-PID and MRAC under actuator fault scenarios.

Figure 1 The Qball-X4 quadrotor UAV (Quanser, 2010)

II. Description and Dynamics of the Quadrotor UAV System

The quadrotor UAV available at the Network Autonomous Vehicle (NAV) Lab in the Department of Mechanical and Industrial Engineering of Concordia University is the Quanser Qball-X4 as shown in **Figure 1**.

The quadrotor UAV is enclosed within a protective carbon fiber ball-shape cage (therefore a name of Qball-X4) to ensure safe operation. It uses four 10×4.7 inch propellers and standard RC motors and speed controllers.

The Qball-X4's proprietary design ensures safe operation and opens the possibilities for a variety of novel applications. The protective cage is a crucial feature since this unmanned aerial vehicle was designed mainly for use in an indoor environment/laboratory, where there are typically many close-range hazards (including other vehicles) and personnel doing flight tests with the Qball-X4. The cage gives the Qball-X4 a decisive advantage over other vehicles that would suffer significant damage if contact occurs between the vehicle and an obstacle.

To obtain the measurement from on-board sensors and to drive the motors connected to the four propellers, the Qball-X4 utilizes Quanser's onboard avionics Data Acquisition Card (DAQ), the HiQ, and the embedded Gumstix single-board micro-computer. The HiQ DAQ is a high-resolution Inertial Measurement Unit (IMU) and avionics Input/Output (I/O) card

designed to accommodate a wide variety of applications. QuaRC, Quanser's real-time control software, allows researchers and developers to rapidly develop and test controllers on actual hardware through a MATLAB/Simulink interface. The open-architecture of QuaRC and extensive Simulink blocksets provide users with powerful control development tools. QuaRC can target the Gumstix embedded computer automatically to generate code and execute controllers on-board the vehicle. During flights, while the controller is executing on the Gumstix, users can tune parameters in real-time and observe sensor measurements from a host ground station computer (PC or laptop).

The user interface to the Qball-X4 is MATLAB/Simulink with QuaRC. The controllers are developed in Simulink environment with QuaRC on the host computer, and these models/controllers are compiled into executable codes and downloaded on the on-board micro-computer (Gumstix) seamlessly. The communication hierarchy and communication diagram as well as the Qball-X4 system configuration is shown in **Figure 2**. For Qball-X4, the following hardware and software are embedded [21]:

- Qball-X4: as shown in **Figure 1**;
- HiQ: QuaRC aerial vehicle Data Acquisition Card (DAQ);
- Gumstix: The QuaRC target single-board microcomputer. An embedded, Linux-based system with QuaRC runtime software installed;
- Batteries: Two 3-cell, 2650 mAh Lithium-Polymer batteries;
- Real-Time Control Software: The QuaRC, a MATLAB/ Simulink configured software as detailed in reference.

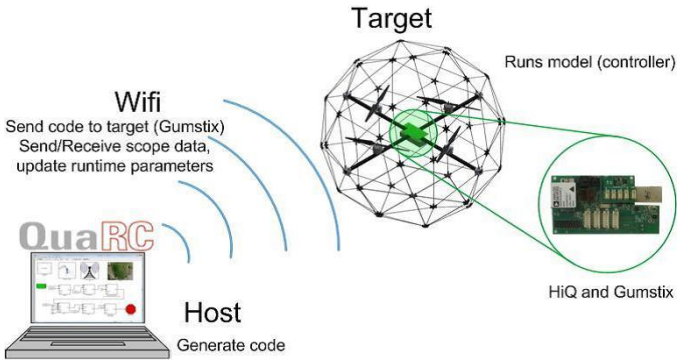

Figure 2 Qball-X4 communication hierarchy and communication diagram

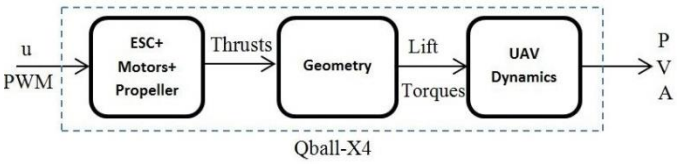

Figure 3 The UAV system block diagram

The block diagram of the UAV system is illustrated in **Figure 3**. It is composed of three main parts. The first part represents the Electronic Speed Controllers (ESCs), the motors, and the propellers in a set of four. The input to this part is $u = [u_1\ u_2\ u_3\ u_4]^T$ which are Pulse-Width-Modulation (PWM) signals. The output is the thrust vector $T = [T_1\ T_2\ T_3\ T_4]^T$ generated by four individually-controlled motor-driven propellers. The second part is the geometry that relates the generated thrusts to the applied lift and torques to the system. This geometry corresponds to the position and orientation of the propellers with respect to the center of mass of the Qball-X4. The third part is the dynamics that relate the applied lift and torques to the position (P), velocity (V) and acceleration (A) of the Qball-X4.

The subsequent sections describe the corresponding mathematical model for each of the blocks in **Figure 3**.

A. Electronic Speed Controllers, DC Motors, and Propellers

The motors of the Qball-X4 are out-runner brushless motors. The generated thrust T_i of the i^{th} motor is related to the i^{th} PWM input u_i by a first-order linear transfer function as follows:

$$T_i = K\frac{\omega}{s+\omega}u_i \qquad (1)$$

where i = 1, 2, 3, 4 and K is a positive gain and ω is the motor bandwidth. K and ω are theoretically the same for the four motors but this may not be the case in practice. It should be noted that u_i = 0 corresponds to zero thrust and u_i = 0:05 ms corresponds to the maximal thrust that can be generated by the i^{th} motor.

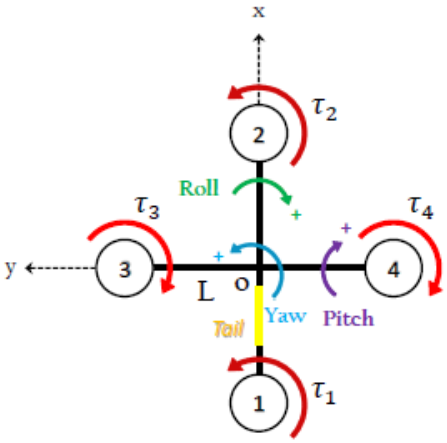

Figure 4 Schematic representation of the Qball-X4

B. Geometry

A schematic representation of the Qball-X4 is given in **Figure 4**. The motors and propellers are configured in such a way that the back and front (1 and 2) motors spin clockwise and the left and right (3 and 4) spin counterclockwise. Each motor is located at a distance L from the center of mass o and when spinning, a motor produces a torque τ_i which is in the opposite direction of that of the motor as shown in **Figure 4**. The origin of the body-fixed frame is the system's center of mass o with the x-axis pointing from back to front and the yaxis pointing from right to left. The thrust T_i generated by the i_{th} propeller is always pointing upward in the z-direction in parallel to the motor's rotation axis. The thrusts T_i and the torques τ_i result in a total lift in the z-direction (body-fixed frame) and torques about the x, y and z axis.

The relations between the lift/torques and the thrusts are

$$\begin{aligned} u_z &= T_1 + T_2 + T_3 + T_4 \\ u_z &= L(T_1 - T_2) \\ u_z &= L(T_3 - T_4) \\ u_z &= \tau_1 + \tau_2 + \tau_3 + \tau_4 \end{aligned} \quad (2)$$

The torque τ_i produced by the i_{th} motor is directly related to the thrust T_i via the relation of $\tau_i = K_\psi T_i$ with K_ψ as a constant. In addition, by setting $T_i = Ku_i$ from (1), the relations (2) can be written in a compact matrix form as:

$$\begin{bmatrix} u_z \\ u_\theta \\ u_\phi \\ u_\psi \end{bmatrix} = \begin{bmatrix} K & K & K & K \\ KL & -KL & 0 & 0 \\ 0 & 0 & KL & -KL \\ KK_\psi & KK_\psi & -KK_\psi & -KK_\psi \end{bmatrix} \begin{bmatrix} u_1 \\ u_2 \\ u_3 \\ u_4 \end{bmatrix} \quad (3)$$

where u_z is the total lift generated by the four propellers and applied to the quadrotor UAV in the z-direction (body-fixed frame). u_θ, u_ϕ, and u_ψ are respectively the applied torques in θ, ϕ, and ψ directions (see **Figure 4**). L is the distance from the center of mass to each motor.

C. *Dynamics of the Quadrotor*

A commonly employed quadrotor UAV model is:

$$\begin{aligned} m\ddot{x} &= u_z(\cos\phi\sin\theta\cos\psi + \sin\phi\sin\psi);\ J_1\ddot{\theta} = u_\theta \\ m\ddot{y} &= u_z(\cos\phi\sin\theta\cos\psi - \sin\phi\sin\psi);\ J_2\ddot{\phi} = u_\phi \\ m\ddot{z} &= u_z(\cos\phi\cos\theta) - mg;\ J_3\ddot{\psi} = u_\psi \end{aligned} \quad (4)$$

where x, y and z are the coordinates of the quadrotor UAV's center of mass in the earth-fixed frame. θ, ϕ, and ψ are the pitch, roll and yaw Euler angles respectively, and m is the mass. If one fixes the yaw angle to zero ($\psi = 0$) and assumes the roll and pitch angles to be very small, then a simplified linear model can be obtained in hovering conditions (u_z = mg in the x and y directions). Therefore the linear model that can be used for control design is given by:

$$\begin{aligned} \ddot{x} &= \theta g;\ J_1\ddot{\theta} = u_\theta \\ \ddot{y} &= -\phi g;\ J_2\ddot{\phi} = u_\phi \\ \ddot{z} &= u_z / m - g;\ J_3\ddot{\psi} = u_\psi \end{aligned} \quad (5)$$

D. *OptiTrack Motion Tracking System for Localization*

A set of twenty four V100:R2 cameras which offers integrated image capture, processing, and motion tracking in a compact package constitute the OptiTrack's optical motion tracking system. The capability of customizing cameras with user-changeable M12 lenses, and OptiTrack's exclusive Filter Switcher technology has let V100 cameras deliver one of the world's premier optical tracking value propositions. Each V100:R2 camera is capable of capturing fast moving objects with its global shutter imager at 100 FPS capture speed. By maximizing its 640×480 Video Graphic Array (VGA) resolution through advanced image processing algorithms, the V100:R2 can also track markers down to sub-millimeter movements with maintainable accuracy [22].

Figure 5 V100:R2 camera used for Optitrack positioning system

A variety of V100:R2 settings are customized with any of OptiTrack's software applications such as the one employed in this study, i.e. Tracking Tool, for greater control over what cameras capture and what information they report to the personal computer set up as the ground station. Available settings include: image processing type, frame rate, exposure, threshold, illumination, filter switching, and status LED control. OptiTrack's application software, named Tracking Tool, interfaces with specific blocks inside MATLAB/Simulink environment within the library of QuaRC. **Figure 5** illustrates one of the six cameras employed constituting the system of OptiTrack.

The following table shows the nominal values of the quadrotor helicopter's system parameters.

m	I_x	I_y	I_z	l	K_{motor}	ω_{motor}
1.4	0.03	0.04	0.03	0.2	120	15
kg	kg.m^2	kg.m^2	kg.m^2	m	N	rad/s

III. GAIN-SCHEDULED PROPORTIONAL-DERIVATIVE-INTEGRAL (GS-PID) CONTROLLER

In view of the advantages of widely used Proportional-Integral-Derivative (PID) controller and gain scheduling control strategy in aerospace and other industrial applications, a simple and practical control strategy by using gain-scheduling based PID controller is proposed for fault tolerant control of the UAV test-bed Qball-X4 for investigating the suitability and capability of such a popular control strategy used for most normal (fault-free) conditions to the cases with faults/damages in the UAV systems. In industrial automation the PID controllers are the standard control strategy thanks to their flexibility of making the PID controllers capable to be used in many situations. Many control problems can be handled very well using PID control. In order to achieve the best performance, the gains of the PID controller must be tuned based on the nature of the plant. The tuning process is the adjustment of the control gains to the optimal values for the desired response. Although tuning of Single-Input-Single-Output (SISO) system PID gains are not very complicated

thanks to several existing tuning methods, the fine-tuning of PID gains for Multi-Input-Multi-Output (MIMO) systems is still challenging. There are some currently existing tuning techniques for PID controllers. The Ziegler-Nichols method is the most well-known method for tuning of PID controllers.

The algorithm of the PID controller for discrete version is shown as following:

$$u(t_k) = u(t_{k-1}) + \Delta u(t_k) \tag{6}$$

where

$$\Delta u(t_k) = K_p\left[e(t_k) - e(t_{k-1})\right] + \frac{K_p h}{T_i} e(t_k) + \frac{K_p T_d}{h}\left[e_f(t_k) - 2e_f(t_{k-1}) + e_f(t_{k-2})\right] \tag{7}$$

where u is the control variable, h is discretization rate, e is the tracking error defined as $e = y_d - y$ where y_d is the desired output and y is the real output of the system. K_p, $K_i = \frac{K_p}{T_i}$, and $K_d = K_p T_d$ are controller gains associated with proportional (P), integral (I), and derivative (D) action, respectively.

Generally, if the change of a dynamics in a system with the operating condition is known, then it is possible to change the parameters of the controller by monitoring the operating conditions of the system. In other words, there are auxiliary variables that relate well to the characteristics of the system dynamics in some systems. If these variables can be measured, they can be used to change the controller parameters. This approach is called as gain scheduling because the scheme was originally used to accommodate changes in plant/system with switching of pre-scheduled controller gains. The block diagram of the Qball-X4 system with gain scheduling control strategy is shown in **Figure 6**.

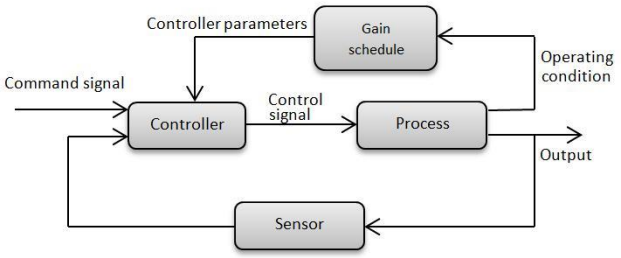

Figure 6 Gain scheduling control structure

The idea of relating the controller parameters to auxiliary variables is not new, but the implementation of gain scheduling is still challenging in practice. Gain scheduling technique has thus been used only in special cases, such as in autopilots for high-performance aircrafts. In fact it is the foremost method for handling parameters variations in flight control systems [10]. Therefore, gain scheduling is a very useful technique for reducing the effects of parameter variations and necessary for fault-tolerant control of a system such as Qball-X4 for handling different fault conditions since a single PID will not work for these different flight conditions. With multiple PIDs and quick and correct switching of the PID controller gains with respect to different fault and operating conditions, a fault-tolerant control system with acceptable performance under fault situations could be achieved. Such a consideration in fact motivated us in this work for investigating and developing gain-scheduled PID control strategy with application to the Qball-X4 UAV under the fault-tolerant control framework with a hope that such a control strategy can work well and practically as the same as the widely used PID in practical engineering applications.

In this work, for GS-PID controller, a set of pre-tuned gains are applied to the controllers under both faultfree and different fault conditions. In order to obtain the best stability and performance of Qball-X4 under both conditions, the switching action from one set of pre-tuned PID gains to another set is highly coupled with the FDD block (shown in 7). Hence, the switching time between the time when fault occurs and the time of switching to a new set of gains plays a vital role. In other words, if this transient (switching) time is held long (more than one second for example) it can cause the Qball-X4 to hit the ground and cause a crash.

The FDD block is designed to detect the fault as quick as possible in order to get the best possible performance of the quadrotor after fault occurrence based on the error between real height (measured by OptiTrack visual system) of the Qball-X4 and the desired height. Since during the flight there exist also disturbances, it was essential to define a threshold for FDD scheme not to be affected by the disturbances. For GS-PID controller, a set of pre-tuned gains are applied to the controllers under both fault-free and fault conditions. In order to obtain the best stability and performance of Qball-X4 under both conditions, the switching action from one set of pre-tuned PID controller gains to another set is required. Different from the conventional gain scheduler under normal (fault-free) system operation, due to the uncertainty on when, where and how significance of a fault to be occurred in a system, the FDD block and the gain scheduler are needed for providing fast and correct switching of pre-tuned PID controller gains when an anticipated fault occurred in the system during system operation. The switching time (or time delay in FDD terminology) plays a vital role in fault accommodation of the Qball-X4. Faster switching time leads to a better stability of the Qball-X4 and more desirable faulttolerant behavior. Development and integration of a FDD scheme with the GS-PID fault-tolerant control to form an active fault-tolerant control system for Qball-X4 is currently under progress as one of future works of this paper. However, effects of time delays in gain switching (FDD decision making) are investigated in this paper through experimental tests.

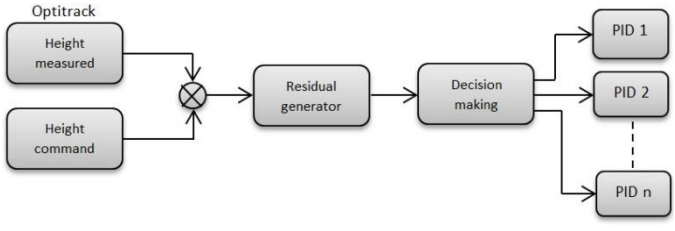

Figure 7 FDD block integrated with GS-PID controller

The testing results are also compared to the single PID controller and the GS-PID controller showed to be fairly reliable with a high reliability, stability and performance of the Qball-X4.

In the next section, the MIT rule-based model reference adaptive control (MRAC) is presented and the experimental testing results for both controllers with fault-free and fault cases are illustrated. Compared with GS-PID, MRAC is a model-based control technique and only linear MRAC control technique is available currently and also investigated in this paper.

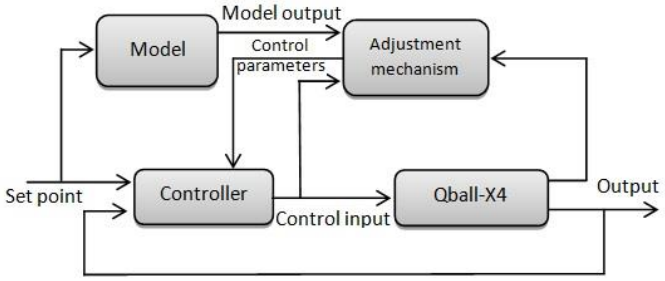

Figure 8 Model reference adaptive control structure

IV. MODEL REFERENCE ADAPTIVE FAULT TOLERANT CONTROLLER

Among all adaptive control techniques the Model Reference Adaptive Systems (MRAS) are important adaptive systems which were originally derived for deterministic continuous-time systems. Extension to discrete time systems and systems with stochastic disturbances has also been carried out. As shown in **Figure 8**, the system has an ordinary feedback loop composed of the plant and the controller and another feedback loop that changes the controller parameters. The parameters are changed on the basis of feedback from the error, which is the difference between the output of the system and the output of the reference model. The ordinary feedback loop is called inner loop, and the parameter adjustment loop is called the outer loop. In other words, Model Reference Adaptive Control (MRAC) is concerned with forcing the dynamic response of the controlled system to asymptotically approach that of a reference system represented by a reference model, despite parametric uncertainties in the system. The mechanism for adjusting the parameters in model reference adaptive system can be obtained by using a gradient method or by applying stability theory [10]. Two major subcategories of MRAC are those of indirect methods, in which the uncertain plant parameters are estimated and the controller redesigned online based on the estimated parameters, and direct methods, in which the tracking error is forced to zero without regarding to parameter estimation accuracy (though under certain conditions related to the level of excitation in the command signal, the adaptive laws often can converge to the proper values). As pointed out in [11], MRAC for linear systems has received, and continues to receive, considerable attention in the literature. Therefore, this paper only investigates linear MRAC techniques.

There are different approaches to MRAC such as [11], and [23]:

- The MIT rule;
- MRAC design based on Lyapunov stability theory;
- Hyperstability and passivity theory;
- The error model;
- Augmented error;
- Model-following MRAC;
- Modified MRAC (M-MRAC);
- Conventional MRAC (C-MRAC);

Although the MIT rule is the original approach to MRAC but it cannot guarantee the stability of the closed-loop controlled system. However, the MRAC based on the Lyapunov stability theory can be considered as an alternative approach. As described in [10], in order to generate MRAC based on Lyapunov's stability theory, first the differential equation of the error which is the difference between the output of the model and the output of the system should be derived which contains the adjustable parameters. In order to reduce the error to zero, a Lyapunov function and an adjustable mechanism should be established. The Lyapunov derivative function *dV/dt* is usually only negative semidefinite. Therefore, to define the parameter convergence, the persistent excitation and the uniform observability should be conducted on the system and the reference signal. The Lyapunov stability theorem for time-invariant systems can be establishes the following: If there exists a function $V: R^n \rightarrow R$ being positive definite and its derivative:

$$\frac{dV}{dt} = \frac{\partial V^T}{dx}\frac{\partial x}{dt} = \frac{\partial V^T}{dx} f(x) = -W(x) \tag{8}$$

is negative semidefinite, then the solution $x(t) = 0$ to

$$\frac{dx}{dt} = f(x), f(0) = 0 \tag{9}$$

is stable. If dV/dt is negative definite the solution will be asymptotically stable. V denotes the Lyapunov function for the system. If:

$$\frac{dV}{dt} < 0 \quad and \quad V(x) \rightarrow \quad when \quad \|x\| \rightarrow \infty \tag{10}$$

the solution is globally asymptotically stable. Therefore, the following procedure was realized: The plant/system model:

$$\ddot{y}_p + a_1\dot{y}_p + a_0 y_p = bu \tag{11}$$

Reference model:

$$\ddot{y}_r + a_1\dot{y}_r + a_0 y_r = b_r u_r \tag{12}$$

The control law:

$$u = \theta_1 u_c - \theta_2 y_p \tag{13}$$

and the error:

$$e = y_p - y_r \tag{14}$$

Then, the error dynamics is represented by:

$$\dot{e} = \dot{y}_p - \dot{y}_r = 1/a_1\left[bu - \ddot{y}_p - a_0 y_p\right] - 1/a_1 r - \left[bu - \ddot{y}_r - a_0 y_r\right] \quad (15)$$

Substituting $y_r = y_p - e$ and $y_r = y_p - e$ from Equation 15, following equation can be derived.

$$\dot{e} = \frac{1}{a_1}bu - \frac{1}{a_1}\ddot{y}_p - \frac{a_0}{a_1}y_p - \frac{1}{a_{r1}}b_r u_c + \frac{1}{a_{1r}}\ddot{y}_p + \frac{1}{a_{1r}}\ddot{e} + \frac{a_{0r}}{a_{1r}}y_p - \frac{a_{0r}}{a_{1r}}e \quad (16)$$

Replacing $u = \theta_1 u_c - \theta_2 y_p$ in the above equation and placing the error terms in the left side of the equation, the following equation is obtained:

$$\frac{1}{a_{1r}}\ddot{e} + \dot{e} + \frac{a_{0r}}{a_{1r}}e = \frac{1}{a_{1r}}b_r\theta_1 u_c - \frac{1}{a_{1r}}b_r u_c - \frac{1}{a_{1r}}b_r\theta_2 y_p + \frac{a_{0r}}{a_{1r}}y_p - \frac{1}{a_1}\ddot{y}_p + \frac{1}{a_{1r}}\ddot{y}_p \quad (17)$$

The Reference Model is equal to the Process Model if no fault occurs ($a_1 = a_{1r}$, $a_0 = a_{0r}$, and $b = b_r$), then:

$$\frac{1}{a_{1r}}\ddot{e} + \dot{e} + \frac{a_{0r}}{a_{1r}}e = \frac{1}{a_{1r}}b_r\theta_1 u_c - \frac{1}{a_{1r}}b_r u_c - \frac{1}{a_{1r}}b_r\theta_2 y_p + \frac{a_{0r}}{a_{1r}}y_p - \frac{1}{a_1}\ddot{y}_p + \frac{1}{a_{1r}}\ddot{y}_p \quad (18)$$

$$\frac{1}{a_{1r}}\ddot{e} + \dot{e} + \frac{a_{0r}}{a_{1r}}e = \frac{1}{a_{1r}}\left(b_r\theta_1 - b_r\right)u_c - \frac{1}{a_{1r}}\left(b_r\theta_2\right)y_p \quad (19)$$

$$\frac{1}{a_{1r}}\frac{d^2e}{dt} + \frac{de}{dt} + \frac{a_{0r}}{a_{1r}}e = \frac{1}{a_{1r}}\left(b_r\theta_1 - b_r\right)u_c - \frac{1}{a_{1r}}\left(b_r\theta_2\right)y_p \quad (20)$$

$$\frac{de}{dt} = -\frac{1}{a_{1r}}\frac{d^2e}{dt} - \frac{a_{0r}}{a_{1r}}e + \frac{1}{a_{1r}}\left(b_r\theta_1 - b_r\right)u_c - \frac{1}{a_{1r}}\left(b_r\theta_2\right)y_p \quad (21)$$

The proposed Lyapunov function is quadratic in tracking error and controller parameter estimation error since it is expected that the adaptation mechanism will drive both types of errors to zero. From the equation error dynamics (see Equation (21)) the proposed Lyapunov function is:

$$V(e,\theta_1,\theta_2) = -\frac{1}{2}\left(a_{1r}e^2 + \frac{1}{\gamma b_r}\left(b_r\theta_1 - b_r\right)^2 + \frac{1}{\gamma b_r}\left(b_r\theta_2\right)^2\right) \quad (22)$$

where b_r, γ and $a_{1r} > 0$. Equation (22) will be zero when the error is zero and the controller parameters are equal to the desired values. The above Lyapunov function is valid if the derivative of this function is negative. Thus, the derivative of Equation (22) is:

$$\dot{V} = a_{1r}e\frac{de}{dt} + \frac{1}{\gamma}\left(b_r\theta_1 - b_r\right)\frac{d\theta_1}{dt} + \frac{1}{\gamma}\left(b_r\theta_2\right)\frac{d\theta_2}{dt} \quad (23)$$

Substituting Equation (21) in the above equation, and rearranging the similar terms, Equation (24) is obtained.

$$\dot{V} = a_{1r}e\left(-\frac{1}{a_{1r}}\frac{d^2e^2}{dt^2} - \frac{a_{0r}}{a_{1r}}e + \frac{1}{a_{1r}}\left(b_r\theta_1 - b_r\right)u_c - \frac{1}{a_{1r}}\left(b_r\theta_2\right)y_p\right) + \frac{1}{\gamma}\left(b_r\theta_1 - b_r\right)\frac{d\theta_1}{dt} + \frac{1}{\gamma}\left(b_r\theta_2\right)\frac{d\theta_2}{dt} \quad (24)$$

$$\dot{V} = -e\frac{d^2e^2}{dt^2} - a_{0r}e^2 + \left(b_r\theta_1 - b_r\right)u_c e - \left(b_r\theta_2\right)y_p e + \frac{1}{\gamma}\left(b_r\theta_1 - b_r\right)\frac{d\theta_1}{dt} + \frac{1}{\gamma}\left(b_r\theta_2\right)\frac{d\theta_2}{dt} \quad (25)$$

$$\dot{V} = -e\frac{d^2e^2}{dt^2} - a_{0r}e^2 + \left(b_r\theta_1 - b_r\right)u_c e + \frac{1}{\gamma}\left(b_r\theta_1 - b_r\right)\frac{d\theta_1}{dt} - \left(b_r\theta_2\right)y_p e - \frac{1}{\gamma}\left(b_r\theta_2\right)\frac{d\theta_2}{dt} \quad (26)$$

$$\dot{V} = -e\frac{d^2e^2}{dt^2} - a_{0r}e^2 + \frac{1}{\gamma}\left(b_r\theta_1 - b_r\right)\left(\frac{d\theta_1}{dt} + \gamma u_c e\right) + \frac{1}{\gamma}\left(b_r\theta_2\right)\left(\frac{d\theta_2}{dt} - \gamma y_p e\right) \quad (27)$$

Therefore, the adaptation parameters are selected to be updated as:

$$\frac{d\theta_1}{dt} = -\gamma u_c e \quad (28)$$

$$\frac{d\theta_2}{dt} = -\gamma y_p e \quad (29)$$

therefore

$$\dot{V} = -e\frac{d^2e^2}{dt^2} - a_{0r}e^2 \quad (30)$$

It can be seen that Equation (30) is negative semidefinite which implies $V(t)V(0)$. This ensures that e, θ_1 and θ_2 are bounded. Since $a_{1r} > 0$, $a_{0r} > 0$ and uc is bounded then yr is bounded and therefore $y_p = e + y_r$ is bounded as well. From the boundedness and convergence set theorem it can be concluded that the error e will go to zero [10].

In this paper, a MIT rule is used to control the height of the Qball-X4. The MIT rule is the original approach to MRAC. The name is derived for the fact that it was developed at the Instrumentation Laboratory at Massachusetts Institute of Technology (MIT) for aerospace applications. However, the schemes based on the MIT rule and other approximations may lead the system becoming unstable.

To present the MIT rule for the design of a MRAC scheme, the system can be considered as follows [24]:

$$\ddot{y}(t) = -a_1\dot{y}(t) - a_2 y(t) + bu(t) \quad (31)$$

where a_1, a_2 and b are unknown system parameters, and $\dot{y}$ and y are available for measurement. The reference model to be matched by the closed-loop system is given by:

$$\ddot{y}_m(t) = -a_{m1}\dot{y}_m(t) - a_{m2}y_m(t) + r(t) \quad (32)$$

where $r(t)$ is the reference command and a_{mi} (i=1; 2) are constants and are chosen based on the performance specifications. The control input $u(t)$ can be defined as follows:

$$u(t) = -\vartheta_1\dot{y}(t) - \vartheta_2 y(t) + r \quad (33)$$

In order to obtain a perfect model following one can substitute Equation (33) into Equation (31) and after differentiating with respect to time, ϑ_1 and ϑ_2 are chosen such that:

$$a_{m1} = a_1 + b\vartheta_1, a_{m2} = a_2 + b\vartheta_2 \quad (34)$$

where a_1 and a_2 and b are assumed to be unknown, thereby the control signal given in Equation (33) is not applicable. Nevertheless, one can use the following $u(t)$:

$$u(t) = -\hat{\vartheta}_1 \dot{y}(t) - \hat{\vartheta}_2 y(t) \tag{35}$$

where $\hat{\vartheta}_i$ $i = 1; 2$ are the estimation of ϑ_i and updated based on the MIT rule. ϑ_1 and ϑ_2 are the parameters to be adjusted by MIT rule to minimize the cost function J. The cost function can be chosen for example as follows:

$$J = \frac{1}{2} e^2 \tag{36}$$

where e is the error showing the difference between the system output and the reference model output i.e. $e = y - y_m$. Hence the parameters should be adjusted in the direction of negative gradient of J:

$$\frac{d\hat{\vartheta}}{dt} = -\gamma \frac{\partial J}{\partial \hat{\vartheta}_i} = -\gamma e \frac{\partial e}{\partial \hat{\vartheta}_i} = -\gamma e \frac{\partial y}{\partial \hat{\vartheta}_i} \tag{37}$$

where $\gamma > 0$ is the adaptation rate and $\frac{\partial e}{\partial \hat{\vartheta}_i}$ is known as sensitivity derivative of the system and is evaluated under the assumption that $\hat{\vartheta}_i$ varies slowly. It should be noted that MRAC designed based on MIT rule is locally stable if γ is small and initial conditions $\hat{\vartheta}_i(0)$ are close to the nominal values of θ_i. Otherwise the aforementioned MIT rule may lead to instability and unbounded signal response. For more details regarding MIT rule readers are referred to [24].

Finally the controller output of the MRAC is fed to the height model of the Qball-X4 as follows:

$$M\ddot{Z} = 4F\cos(\phi)\cos(\theta) - Mg \tag{38}$$

and the experimental testing results will be shown in the next section. It is worth to mention that the MRAC control design values are set as: $a_{m1} = 2$, $a_{m2} = 2$ and $\gamma = 0{:}04$.

V. EXPERIMENTAL TESTING RESULTS

In this section, experimental testing results are shown based on the above GS-PID and MRAC controllers under fault-free and a fault condition with an 18% of power loss in all motors occurred at 30 second.

A. Experimental Testing Results with GS-PID

For PID controllers, it can be seen in **Figure 9** that the single PID controller, which is tuned well for normal take-off and hovering, is not able to handle the faulty situation that is set to 18% of power loss in all motors. However, as can be seen from **Figsures 10, 11** and **12**, the GS-PID controller can handle the fault and results in better height hold than the single PID controller even with certain time delays in control gains switching. The best performance with GS-PID controller is presented in **Figure 10** which shows the ideal matched cooperation of FDD block along with GS-PID controller.

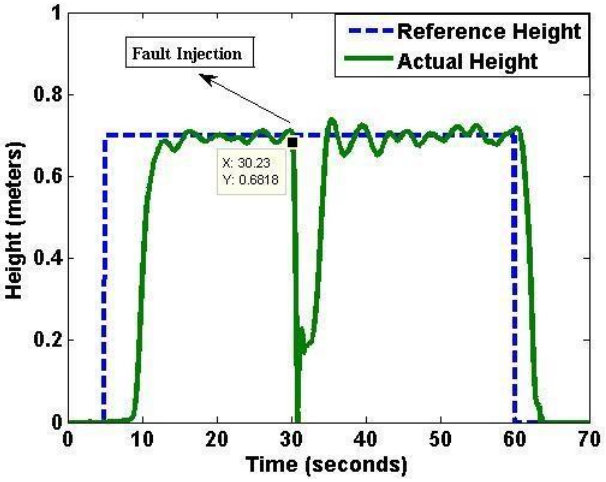

Figure 9 Single PID controller in the presence of an 18% of fault on all actuators

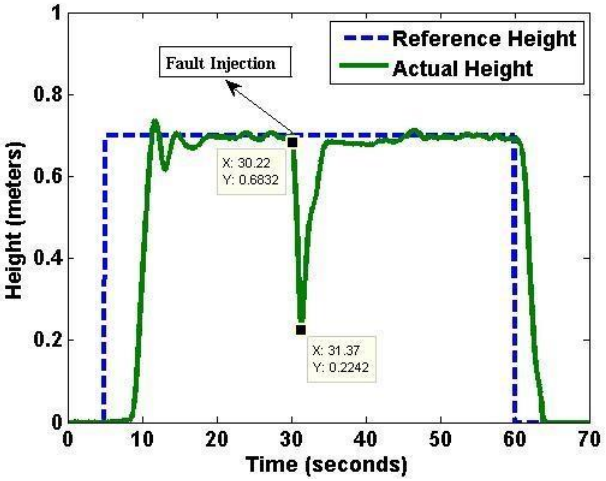

Figure 10 Simultaneous fault injection and gains switching of GS-PID in the presence of an 18% of fault on all actuators

As mentioned before the fault occurrence and detection time is vital for the stability and the acceptable performance of the Qball-X4. Comparisons with time delay of 0.5s and 1s are shown in **Figures 11** and **12**, respectively. Better performance with a shorter time delay of 0.5s has been achieved which verified the importance of fast and correct fault detection and control switching (reconfiguration) after fault occurrence.

If the fault occurrence and the switching of controller gains occurs at the same time, i.e. with the perfect fault detection and diagnosis, the best result will be achieved for the GS-PID as shown in **Figure 10**.

It should be mentioned that since only height control is implemented by GS-PID, a Linear Quadratic Regulator (LQR) with Integral Action (LQR-IC) controller is also used to control the pitch and roll motion of the unmanned quadrotor helicopter during the experimental tests.

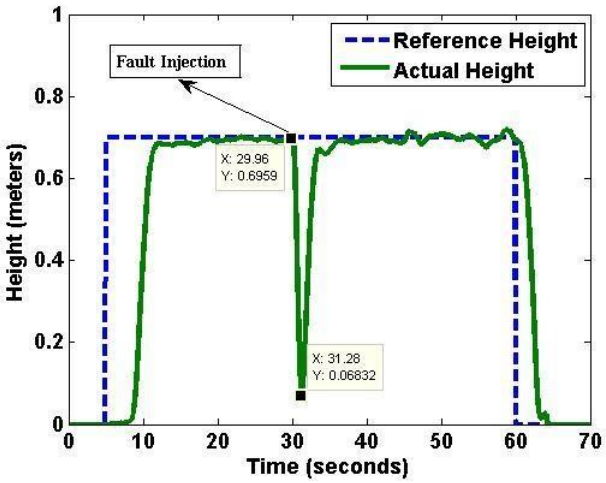

Figure 11 GS-PID control with 0.5s time-delay in controller gains switching after the fault occurrence

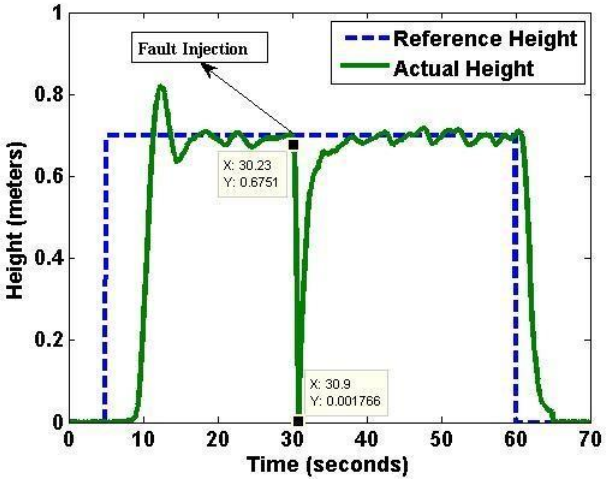

Figure 12 GS-PID control with 1s time-delay in controller gains switching after the fault occurrence

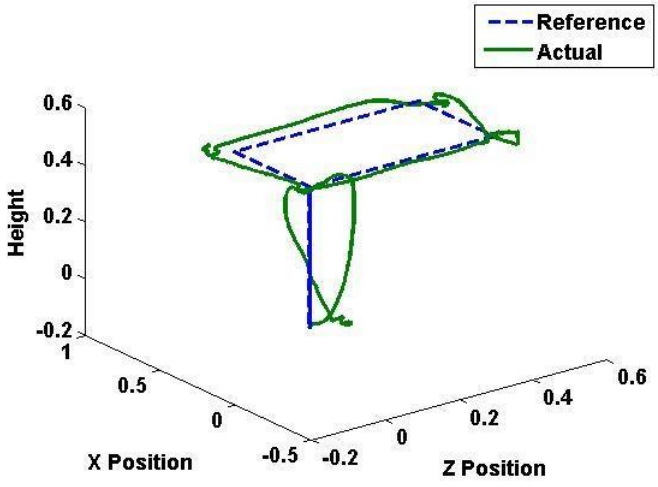

Figure 13 Square trajectory in fault-free condition with MRAC

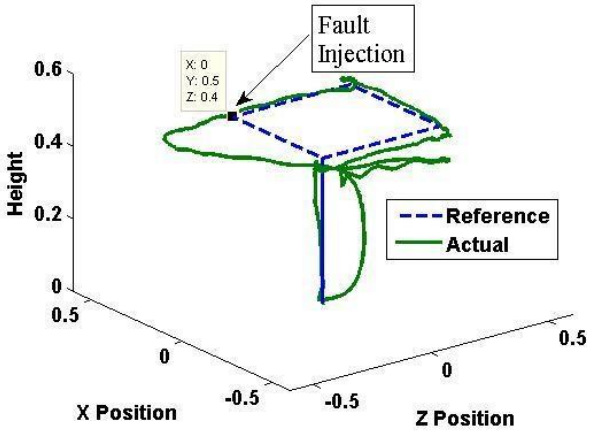

Figure 14 Square trajectory in faulty condition with MRAC

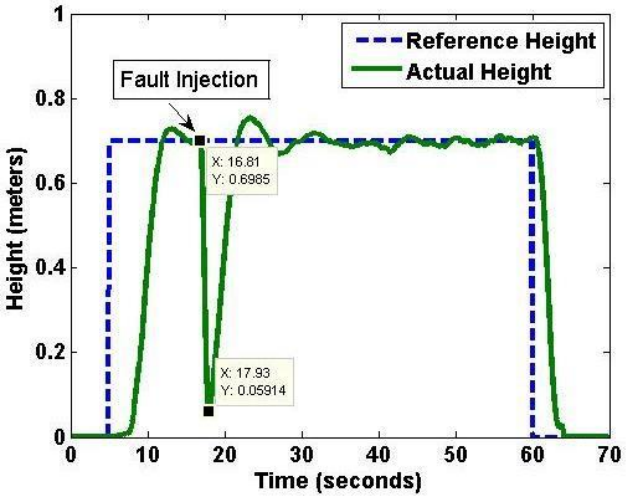

Figure 15 MRAC with an 18% fault in all motors

B. Experimental Testing Results with MRAC

For MRAC, hovering control and trajectory tracking control scenarios with injected fault are applied to Qball-X4 and the experimental testing results are shown as in **Figures 12-14**.

In **Figure 13**, the trajectory tracking to 0.5 m x 0.6 m square trajectory under fault-free condition is shown, while the trajectory tracking performance under a fault scenario with faults injected only to forward (rotor #1) and left (rotor #3) actuators at 50 second with a 12% control effectiveness loss is shown in **Figure 14**.

As can be seen from **Figure 14** the real trajectory of the Qball-X4 deviates from the desired path immediately after the occurrence of the fault.

For easy comparison with GS-PID, **Figure 15** shows the height control based on the MRAC when an 18% control effectiveness loss in all motors occurred at 17 second. It can be seen that the Qball-X4 was able to accommodate the fault before touching the ground. Deviation from the desired height is larger than the case of GS-PID shown in Fig. 10, but similar to the case in Fig. 11 with 0.5 second time delay in the GS-PID.

C. Comparison Between GS-PID and MRAC

As mentioned previously, two typical control techniques (model-free: GS-PID and model-based: MRAC) are applied to Qball-X4 quadrotor helicopter in this work. MRAC showed a promising performance for handling the fault for all actuators as well as a good faultfree performance. On the other hand the GS-PID was able to handle the fault better than MRAC in the sense of controller reactions and ability to keep the height. In other words the GS-PID showed more capability than the MRAC to keep the height of the helicopter if the faster or instantaneous switching of the GS-PID controller gains after fault occurrence can be achieved with a fast fault detection and diagnosis scheme. However, delay in detection and controller switching (or reconfiguration) should always exist in practical applications, although it could be very small. Effect and criticality of time delays to the overall system depends also on the flight conditions and particular applications.

VI. CONCLUSION AND FUTURE WORK

In this paper, two types of popular controllers, Proportional-Integral-Derivative (PID) controller with Gain Scheduling (GS) technique and Model Reference Adaptive Control (MRAC), have been developed; experimentally flying tested, and compared with application to a physical quadrotor helicopter UAV test-bed. Both controllers showed good results for height control of the quadrotor UAV: Qball-X4. Unlike the GS-PID, the single PID which is tuned for normal flight was not able to handle faults with larger fault severity.

The future work is considered to apply gain scheduling Linear Parameter Varying (LPV) technique to the same testbed, since there is no stability guarantee for nonmodel based switching controllers such as GS-PID. With the help of LPV technique it is possible to increase the stability and performance of the system for actuator fault-tolerant control cases.

ACKNOWLEDGMENT

This work is financially supported by the Natural Sciences and Engineering Research Council of Canada (NSERC) through a Strategic Project Grant and a Discovery Project Grant led by the third author. Support from Quanser Inc. and colleagues from Quanser Inc. for the development of the Qball-X4 UAV test-bed is also highly appreciated.

NOMENCLATURE

ω	bandwidth of actuator
M	mass
L	quadrotor arm length
τ	torque
F	force
T	thrust generated by each motor
a_1, a_2, b	unknown plant model parameters
J	cost function
K	actuator's positive gain
ϕ, θ	roll and pitch

REFERENCES

[1] Y. Zhang and J. Jiang, "Bibliographical review on reconfigurable fault-tolerant control systems," Annual Review in Control, vol. 15, no. 32-2, pp. 229–252, 2008.

[2] R. Isermann, Ed., Fault-Diagnosis Systems. Sptinger-Velrage, Berlin Heidelberg, 2006. CrossRef

[3] G. J. Ducard, Ed., Fault-tolerant Flight Control and Guidance Systems. Springer, 2009. CrossRef

[4] E. N. Johnson, G. V. Chowdhary, and M. Kimbrell, "Guidance and control of an airplane under severe structural damage," AIAA Infotech@Aerospace, Atlanta, Georgia, USA, 2010. CrossRef

[5] A. Bani Milhim, Y. M. Zhang, and C. A. Rabbath, "Gain scheduling based pid controller for fault tolerant control of a quad-rotor uav," AIAA InfotechAerospace, Atlanta, Georgia, USA, 2010.

[6] H. Amoozgar, A. Chamseddine, and Y. Zhang, "Fault-tolerant fuzzy gain-scheduled pid for a quadrotor helicopter testbed in the presence of actuator faults," IFAC Conference on Advances in PID Control, Brescia, Italy, 2012.

[7] A. Salih, M. Moghavvem, H. Mohamed, and K. Gaeid, "Flight pid controller design for a uav quadrotor," Scientific Research and Essays, vol. 5, no. 23, pp. 3660–3667, 2010.

[8] S. Bouabdallah and R. Noth, A. Siegwart, "PID vs LQ control techniques applied to an indoor micro quadrotor," Proc. of The IEEE International Conference on Intelligent Robots and Systems (IROS), vol. 3, 2004. CrossRef

[9] A. Wahyudie, T. B. Susilo, and H. Noura, "Robust PID controller for quad-rotors," Journal of Unmanned System Technology, vol. 1, pp. 14–19, 2013.

[10] K. J. Astrom and B. Wittenmark, Eds., Adaptive Control. Dover, 2008.

[11] B. T. Whitehead and S. R. Bieniawskiy, "Bibliographical review on reconfigurable fault-tolerant control systems," Annual Review in Control, vol. 15, no. 32-2, pp. 229–252, 2008.

[12] R. Gadient, J. Levin, and E. Lavretsky, "Bibliographical review on reconfigurable fault-tolerant control systems," Annual Review in Control, vol. 15, no. 32-2, pp. 229–252, 2008.

[13] J. Guo and G. Tao, "A multivariable mrac design for aircraft systems under failure and damage conditions," Proceedings of American Control Conference, 2011.

[14] K. A. Lemon, J. E. Steck, and B. T. Hinson, "Model referece adaptive flight control adapted for general aviation: Controller gain simulation and preliminary flight testing on a bonanza fly-by-wire testbed," 2010.

[15] P. J. and N. M.J., "Design of a model reference adaptive controller using modified mit rule for a second order system," Advance in Electronic and Electric Engineering, vol. 3, no. 4, pp. 477–484, 2013.

[16] P. Swarnkar, S. Jain, and R. Nema, "Effect of adaptation gain in model reference adaptive controlled second order system," vol. 1, no. 3, pp. 70–75, 2011.

[17] L. Zheng, "Model reference adaptive controller design based on fuzzy inference system," Information Computational Science, vol. 9, no. 8, pp. 1683–1693, 2011.

[18] T. N. Nguyen, K. Krishnakumar, and J. Bokovic, "An optimal control modification to modelreference adaptive control for fast adaptation," AIAA Guidance, Navigation and Control Conference, 2008.

[19] N. Golea, A. Golea, and M. Kadjoudj, "Nonlinear model reference adaptive control using takagisugeno fuzzy systems," Intelligent Fuzzy Systems, no. 17, pp. 47–57, 2006.

[20] J. Lee, B. Suh, and K. Abi, "Model reference adaptive control of nonlinear system using feedback linearization," SICE '95. Proceedings of the 34th SICE Annual Conference, pp. 1571–1576, 1995.

[21] Quanser Inc., "Qball manual, 2010. VIEW

[22] Optitrack, 2016 VIEW

[23] Z. T. Dydek and A. M. Annaswamy, "Combined/composite adaptive control of a quadrotor uav in the presence of actuator uncertainty," AIAA Guidance, Navigation, and Control Conference, Toronto, Ontario, Canada, 2010. CrossRef

[24] A. Chamseddine, Y. M. Zhang, C. A. Rabbath, C. Fulford, and J. Apkarian, "Model reference adaptive fault tolerant control of a quadrotor uav," Infotech@Aerospace, St. Louis, Missouri, USA, 2011. CrossRef